The pathway of aerosol direct effects impact on secondary inorganic aerosol formation

Jiandong Wang[1,2], Jia Xing[2*], Shuxiao Wang[2], Rohit Mathur[3], Jiaping Wang[4], Yuqiang Zhang[5], Chao Liu[1], Jonathan Pleim[3], Dian Ding[2], Xing Chang[2], Jingkun Jiang[2], Peng Zhao[6], Shovan Kumar Sahu[2], Yuzhi Jin[1], David C. Wong[3], Jiming Hao[2]

[1]Key Laboratory for Aerosol-Cloud-Precipitation of China Meteorological Administration, School of Atmospheric Physics, Nanjing University of Information Science and Technology, Nanjing, 210044, China

[2]State Key Joint Laboratory of Environmental Simulation and Pollution Control, School of Environment, Tsinghua University, Beijing, 100084, China

[3]The U.S. Environmental Protection Agency, Research Triangle Park, NC, 27711, U.S.A

[4]Jiangsu Provincial Collaborative Innovation Center for Climate Change, School of Atmospheric Science, Nanjing University, Nanjing, 210023, China

[5]Nicholas School of the Environment, Duke University, Durham, NC, 27710, U.S.A

[6]Department of Health and Environmental Sciences, Xi'an Jiaotong-Liverpool University, Suzhou, 215123, China

Correspondence to: Jia Xing (xingjia@mail.tsinghua.edu.cn)

Abstract. Airborne aerosols reduce surface solar radiation through light scattering and absorption (aerosol direct effects, ADE), influence regional meteorology, and further affect atmospheric chemical reactions and aerosol concentrations. The inhibition of turbulence and the strengthened atmospheric stability induced by ADE increases surface primary aerosol concentration, but the pathway of ADE impacts on secondary aerosol is still unclear. In this study, the online-coupled meteorological and chemistry model (WRF-CMAQ) with integrated process analysis was applied to explore how ADE affects secondary aerosol formation through changes in atmospheric dynamics and photolysis processes. Meteorological condition and air quality in Jing-Jin-Ji area (denoted JJJ, including Beijing, Tianjin and Hebei Province in China) in January and July 2013 were simulated to represent winter and summer conditions, respectively. Our results show that ADE through photolysis pathway inhibits sulfate formation during winter in the JJJ region and promotes sulfate formation in July. The differences are attributed to the alteration of effective actinic flux affected by single scattering albedo (SSA). ADE through dynamics pathway acts as an equally or even more important route compared with photolysis pathway in affecting secondary aerosol concentration in both summer and winter. ADE through dynamics traps formed sulfate within planetary boundary layer (PBL) which increases sulfate concentration in winter. Meanwhile, the impact of ADE through dynamics is mainly reflected in the increase of gaseous precursors concentrations within PBL which enhances secondary aerosol formation in summer. For nitrate, reduced upward transport of precursor restrains the formation in high altitude and eventually lower the nitrate concentration within PBL in winter, while such weakened vertical transport of precursor increases nitrate concentration within PBL in summer since nitrate is mainly formed near surface ground.

1 Introduction

Aerosols have long been recognized as a major source of uncertainty in the climate system (Carslaw et al., 2013;Koch and Del Genio, 2010;Ramanathan et al., 2001;Rosenfeld et al., 2014). It perturbs the Earth's energy budget through aerosol direct effects (ADE) by direct scattering and absorbing shortwave and longwave radiation and indirect effects via interaction with cloud. Besides the climatic effects, studies in recent decades have revealed that it alters regional weather (Sun and Zhao, 2021; Zhao et al., 2018, 2020). Airborne aerosols can alter planetary boundary layer (PBL) development (Atwater, 1971;Ackerman, 1977;Ramanathan et al., 2001;Wendisch et al., 2008;Grell et al., 2011;Wong et al., 2012;Barbaro et al., 2013; Wang et al., 2013) and further deteriorate air quality, which is defined as aerosol-PBL interactions. (Ding et al., 2013; Wang et al., 2014;Xing et al., 2015a;Xing et al., 2016;Wang et al., 2018b;Wang et al., 2015; Yang et al., 2016a; Hong et al., 2020). Absorption and scattering of aerosols reduce the solar radiation reaching to the ground which lower the surface temperature (McCormick and Ludwig, 1967;Li et al., 2015; Yang et al., 2016b, 2018). Meanwhile, aerosols can heat up the air in upper-layer with the presence of absorbing components (black carbon, brown carbon and dust)(Ding et al., 2016b; Huang et al., 2018;Wang et al., 2018a). Such controversial effects modify the vertical temperature profile and suppress the development of PBL, resulting in accumulation of pollutants in near-surface layer and aggravation of atmospheric pollution (Huang and Ding, 2021).

Compared to the impact pathways of ADE on primary aerosol through inhibition of PBL development, ADE effects on secondary aerosol, which is formed in the atmosphere through atmospheric reaction, are much more complicated. ADE can affect secondary aerosol by changing vertical/horizontal transport and altering its precursors and reaction rate (Li et al., 2017;Liao et al., 2015;Ding et al., 2016a;Yang et al., 2017). Studies have been conducted to explain the impact of aerosol on atmospheric oxidations through attenuation. He and Carmichael (1999) illustrated the distinct roles of different types of aerosols on photochemical reaction rate and ozone (O_3) concentration. Atmospheric aerosols cause significant attenuation of ultraviolet radiation and affect photolysis rates and species chemical cycles (Deng et al., 2012; Mok et al., 2016). Zheng et al. (2015) showed that oxidant concentrations fall dramatically during high aerosol loading in winter, suggesting a reduction in secondary aerosols through gaseous reactions. However, impacts of ADE on secondary particle formation through atmospheric dynamic processes have not been well studied. Reduced ventilation by ADE will concentrate gaseous precursors thereby changing secondary particle formation in surface and upper layers and indirectly influencing the aerosol concentration. Additionally, since secondary aerosol could either form in upper layers and get transported to near-ground level or form in near-ground level and get transported aloft, the modulation of PBL development due to ADE may either increase or decrease surface-level secondary aerosol concentrations. A detailed understanding of the physical processes causing these impacts on near-surface and free tropospheric aerosol burden and their quantification are still needed as is the relative importance of each pathway and their likely seasonal variation. To gain further insight into these pathways, process analysis is conducted in this study.

With the rapid development of the economy and the acceleration of urbanization, air quality in China has been deteriorating in recent decades and extreme air pollution events have occurred frequently across China (Wang et al., 2018a). In 2010, the population-weighted $PM_{2.5}$ concentration in China was as high as 59 $\mu g/m^3$. More than 80% of the residents live in regions where 5-year averaged $PM_{2.5}$ is above the national Class II regional air quality standards (i.e., more than 35 $\mu g/m^3$) (Apte et al., 2015). In 2013, annual-averaged $PM_{2.5}$ concentrations across 74 key cities in China ranged from 26 to 160 $\mu g/m^3$, with many locations far exceeding China's air quality standard. The number of premature deaths due to exposure to $PM_{2.5}$ in China is estimated to be more than 1 million for 2010 conditions (Wang et al., 2017;Lim et al., 2012;Apte et al., 2015). The air quality in China has improved significantly since 2013, owing to the strict control acts in China (Fan et al., 2020; Zhang et al., 2020). But understanding the causes of heavy pollution incidents is needed for developing effective pollution control measures in China. To provide an insight into these questions, this study analyzes the contribution of each pathway for secondary inorganic aerosols. The diurnal and seasonal variations in these pathways are also explored. Investigation on the influence of ADE on atmospheric pollution will provide important guidance for understanding the cause of atmospheric pollution and developing effective control strategies.

2 Methods

The overall modeling methodology for the study is detailed previously in Xing et al. (2017) and is briefly summarized here. In this study, the two-way coupled WRF-CMAQ meteorology-chemistry-transport model (Wong et al., 2012) was used to simulate the ADE impacts. Meteorology was simulated by the Weather Research and Forecasting Model (WRF) version 3.4 developed by the National Center for Atmospheric Research (NCAR). Meteorological input data were the National Environmental Prediction Center (NCEP) / NCAR reanalysis data. The Pleim-Xiu land surface model (Pleim and Xiu, 2003; Pleim and Gilliam, 2009), associated with Asymmetric Convective Model of version 2 (ACM2) PBL scheme was used in this study. MODIS land-use type was chosen. RRTMG radiation parameterization scheme was used for shortwave and longwave radiation treatment. The Morrison 2-Moment microphysics scheme and Kain-Fritsch cumulus scheme were used in this study. NCEP Automated Data Processing (ADP) global surface and upper-air observation data were carried out for four-dimensional Data assimilation (Grid FDDA). The air quality model used in this study was the Community Multiscale Air Quality Modeling System (CMAQ) version 5.0.1, developed by the Environmental Protection Agency of the United States. In our previous papers, we have detailed and fully evaluated the model (Xing et al., 2015a; Xing et al., 2015b; Wang et al., 2014; Xing et al., 2017). The comparison of simulated and observed $PM_{2.5}$ concentration is shown in Fig. S1 in supplemental information. Gaseous species and aerosols were simulated by using Carbon Bond 05 (CB05) gas-phase chemistry (Sarwar et al., 2008) with AERO6 aerosol module (Appel et al., 2013). The BHCOAT coated-sphere module (Bohren and Huffman, 1983) was used to simulate aerosol optical properties based on simulated aerosol composition and size distribution (Gan et al., 2015). The gridded emission inventory, initial and boundary conditions used in this study were consistent with our previous studies (Wang et al., 2011;Zhao et al., 2013b;Zhao et al., 2013a;Wang et al., 2014).

Figure 1 shows the modelling domain, which covers most of China and surrounding portions of East Asia, discretized with a 36 km × 36 km grid resolution. WRF and CMAQ both use 23 vertical layers, in which 8 layers are set under 1 km to better describe the boundary layer processes. January 1st to 31st and July 1st to 31st in 2013 were selected to represent winter and summer conditions, respectively. Each simulation was also preceded by a 7-day spin-up period. Jing-Jin-Ji area (denoted JJJ), including Beijing, Tianjin and Hebei Province in China, were selected for the analysis. In this study, observation data from the China National Urban Air Quality Real-time Publishing Platform supported by Ministry of Ecology and Environment, China was used to evaluate the model performance. The validation results were shown as Fig. S1 to Fig. S4 in supplemental information.

Following our previous analyses (Xing et al., 2017), three scenarios were simulated, including 1) the baseline simulation (denoted SimBL) in which no aerosol did not change photolysis rates or dynamics were considered, 2) the simulation (denoted SimNF) in which aerosol only affects photolysis rates, and 3) the simulation (denoted SimSF) in which aerosol feedbacks were considered through both photolysis and dynamic processes. The differences between the simulations of SimNF and SimBL were used to present the ADE impacts through photochemistry process (ADEP, denoted Photolysis in the figures). Similarly, the differences between the simulations of SimSF and SimNF were used to estimate the ADE impacts through dynamic process (ADED, denoted Dynamics in the figures). The combined ADE impacts due to both photolysis and dynamics (denoted ΔTotal) were estimated from the differences between the simulations of SimSF and SimBL.

To further explore these impacts, Process Analysis (PA) technology (Gipson and Young, 1999) was applied in the simulation of WRF-CMAQ (Xing et al., 2011). Eulerian chemistry transport model simulates air pollution concentration by solving transport partial differential equations. A series of physical and chemical processes is calculated to determine the changes in species concentration at each timestep. Based on the properties of linear equation, process analysis could estimate the accumulated effects of each process. The Integrated Process Rates (IPRs) quantify the hourly tendencies from six major modelled atmospheric processes shaping the simulated aerosol concentrations. These process tendencies represent the dominant sinks or sources and include aerosol process (denoted AERO), cloud processes (i.e., the net effect of cloud attenuation of photolytic rates, aqueous-phase chemistry, et al., denoted CLDS), dry deposition (denoted DDEP), horizontal advection (denoted HADV), horizontal diffusion (denoted HDIF), vertical advection (denoted ZADV), and vertical diffusion (denoted VDIF). We combined VDIF, ZADV, and DDEP as vertical transport (VTRN) and combined HDIF and HADV as horizontal transport (HTRN).

3 Results and Discussions

The perturbation of ADE on solar radiation and PBL is presented in Fig. 2 and Fig. 3, respectively. As shown in Fig. 2, ADE reduces solar radiation reaching the ground. The daily maximum reduction occurs at noon, with a mean value of 70 W/m^2 and 40 W/m^2 in January and July, respectively. Decreased solar radiation weakens surface turbulence and reduces the daily maximum PBL height. Figure 3 illustrates that the impact of ADE on monthly mean PBL height shows a unimodal distribution in January and bimodal distribution in July. The PBL height is reduced mostly in the afternoon. The daily average reduction in January and July is about 70 m and 30 m, respectively. Meanwhile, the daily maximum PBL heights are about 500 m and 1500 m in January and July, respectively. It indicates that the change of PBL height is more significant in January.

To provide insight into how ADE affects sulfate concentration, the vertical distribution of sulfate concentration and related processes response to ADE is presented in Fig. 4 and Fig. 5. As shown in Fig. 4, ADE affects sulfate through both photolysis and dynamics in January, leading to a decrease of sulfate formation rate in all layers. The reduction rate due to ADEP is about 3% on average in the near surface layer. Dynamic processes lead to an increase in sulfate concentration in the near surface layer and a decrease of sulfate concentration above 300 m. These two processes combined contribute a 7.5% reduction of sulfate at 900 m, which is the strongest affected layer in terms of sulfate concentration. In July, the ADED is the key process altering sulfate concentration. The strongest impact is at 1100 m. Traditionally, the pathway through changing of actinic flux is emphasized, but the pathway through dynamic process and further change of gaseous precursors are barely mentioned. Our results indicate that ADE affecting sulfate formation through dynamic pathway is equally or even more important than that of photolysis pathway in both summer and winter.

The vertical distribution of the sulfate IPRs response to ADE is presented in Fig. 5. The vertical profile at noon is chosen to discuss here since it has the strongest sulfate formation and ADE impact on solar radiation. The influence of ADEP in January is mainly reflected in the reduction of sulfate formation (AERO, Fig. 5a red). This effect occurs at almost all altitudes and is greater at lower altitudes. ADED is mainly reflected in the weakening vertical transport (VTRN) of sulfate (Fig. 5b purple) caused by shallower PBL. Further, the weakening VTRN caused by ADED results in an increase of sulfate concentration below 500m and decreased sulfate concentration above 500m. The dividing point is at a similar altitude to daily max PBL height. Moreover, the dynamic path barely changes the AERO process (Fig. 5b red). It implies that the ADED affects sulfate concentration mainly by trapping sulfate in the near surface layer rather than changing SO_2 concentration and sulfate formation. Compared with winter, ADED changes sulfate by promoting sulfate formation in July (Fig. 5e, red and green). ADEP on aerosol formation is negative in winter but positive in summer (Fig. 5d, red). This is mainly due to the different role of light-absorbing and scattering aerosols in photolysis. Usually, scattering aerosol increases the optical path length and raises the total actinic flux in the atmosphere as a whole, while absorbing aerosol decreases the actinic flux in the layer below (Dickerson et al., 1997;Herman et al., 1999). In winter, coal combustion and biomass burning, especially for residential heating, leads to high levels of light-absorbing carbon, which results in decreased actinic flux and weakened sulfate formation. Contrarily, lower fraction of light-absorbing aerosol increases actinic flux, promoting sulfate formation in July.

The results above indicate that solar radiation is the restricting factor in winter, and the formation of sulfate is sensitive to the perturbation of solar radiation. In summer, solar radiation is abundant and sulfate formation is primarily limited by availability of gaseous precursors. Diurnal variation of sulfate formation further verifies above speculation. Fig. 6 shows that ADEP inhibits surface sulfate formation during daytime in January, since aerosol with low SSA and long optical path length reduces the actinic flux. In July, ADEP restrains sulfate formation in early morning and late afternoon yet slightly promotes sulfate formation at noon. Along with the strong ADED effects, sulfate formation is promoted from 10:00 to 15:00 local time in summer.

The ADE impacts on nitrate are then investigated. Vertical profile of nitrate affected by ADE is presented in Fig. 7. Overall, ADED makes stronger influence on nitrate concentration than ADEP in both winter and summer. ADEP slightly reduces nitrate concentration near surface in both seasons (Fig. 7a and 7d). As for ADED, it generally lowers the nitrate concentration in winter (Fig. 7b) and the largest reduction occurs above PBL (at around 900 m). During summer, ADED exhibits a promotion effect on nitrate, especially in near surface layers (Fig. 7e). The reason of such different impact of ADED is caused by the

opposite transport direction in January and July (Fig. 8). As shown in Fig. 8, nitrate is mainly formed at high altitude due to the lower temperature in January and is entrained to the surface with PBL development, which is also noted in previous studies (Huang et al., 2021;Curci et al., 2015). Meanwhile, the suppressed PBL reduces the upward transport of NO_x (major precursor of nitrate), resulting in weakened nitrate formation at around 900 m in winter. Conversely, the transport direction of nitrate is bottom-up in July. Therefore, restrained upward transport of NO_x increases the formation of nitrate in near surface layer.

The vertical distribution of the nitrate IPRs response to ADE is presented in Fig. 9. ADEP increases nitrate consumption (AERO, Fig 9a red) in the near ground layer in January while it barely changes the nitrate formation in July (Fig. 9d, red). In general, ADED is dominant in the upper layers in January and in all layers in July. ADED affects nitrate concentration through two major pathways, i.e., vertical transport (shown in Fig. 9b and 9e, purple) and precursor concentration with further impact on formation (shown in Fig. 9b and 9e, red). During winter, AERO is the main sink in the near ground levels and the transport direction is top-down. Decreased nitrate formation (Fig 9b, red) outside PBL and suppressed PBL results in weakened vertical transport of nitrate (Fig 9e, purple) and decrease of its concentration within PBL. In summer, AERO is the main source and VTRN is the major sink. The main reason for increased nitrate concentration is that the accumulation of gaseous precursor in PBL enhances nitrate formation (Fig 9e, red). This effect further increases the absolute amount of nitrate transportation.

4 Conclusions

In addition to directly deteriorating air quality, aerosol diminishes solar radiation due to light scattering and absorption thereby influencing regional meteorology and further modulating air quality. The impact of ADE on secondary aerosol is more complicated than primary aerosol. This study quantified the impacts of ADE on secondary inorganic aerosol using the two-way online coupled meteorology and atmospheric chemistry model (WRF-CMAQ) with integrated process analysis. The main pathways through which ADE affects aerosol concentrations were examined. The key conclusions are 1) ADE reduces solar radiation and decreases PBL height, trapping aerosol in near ground layers. Including ADE improves the model performance for simulating $PM_{2.5}$ and its components. 2) ADE through photolysis pathway inhibits sulfate formation during winter in the JJJ region and promotes sulfate formation in July. The differences are attributed to the alteration of effective actinic flux affected by AOD, solar zenith angle and SSA. 3) ADE through dynamics pathway acts as an equally or even more important route compared with photolysis pathway in affecting secondary aerosol concentration in both summer and winter. 4) ADE through dynamics traps formed sulfate within PBL which increases sulfate concentration in winter. Meanwhile, the impact of ADE through dynamics is mainly reflected in the increase of gaseous precursors concentrations within PBL which enhances secondary aerosol formation in summer. 5) Reduced upward transport of precursor restrains the formation of nitrate in high altitude and eventually lower the nitrate concentration within PBL in winter, while such weakened vertical transport of precursor increases nitrate concentration within PBL in summer since nitrate is mainly formed near surface ground.

Author contributions: J.D.W, J.X and J.P.W. wrote the manuscript with inputs from all co-authors. J. X. and J.D.W. performed the simulation and analyzed the data. D.D. and D. W. supported the model configuration and simulation. S.W., R.M., Y.Z., J.E.P., X.C., J.J., P.Z., S.S., Y.J., and J.H. discussed the results and commented on the manuscript.
Data availability: Model outputs are available upon request from the corresponding author.

Acknowledgements

This work was supported in part by National Science Foundation of China (42075098 & 41907190), National Key R&D program of China (2018YFC0213805). This work was completed on the “Explorer 100” cluster system of Tsinghua National Laboratory for Information Science and Technology.
Competing interests: The authors declare that they have no conflict of interest.

Disclaimer: The views expressed in this paper are those of the authors and do not necessarily represent the view or policies of the U.S. Environmental Protection Agency.

References

Ackerman, T. P.: A Model of the Effect of Aerosols on Urban Climates with Particular Applications to the Los Angeles Basin, J Atmos Sci , 34, 531-547, doi:10.1175/1520-0469(1977)034<0531:amoteo>2.0.co;2, 1977.

Appel, K., Pouliot, G., Simon, H., Sarwar, G., Pye, H., Napelenok, S., Akhtar, F., and Roselle, S.: Evaluation of dust and trace metal estimates from the Community Multiscale Air Quality (CMAQ) model version 5.0, Geosci Model Dev., 6, 883-899, doi: 10.5194/gmd-6-883-2013, 2013.

Apte, J. S., Marshall, J. D., Cohen, A. J., and Brauer, M.: Addressing Global Mortality from Ambient PM2.5, Environ. Sci. Technol., 49, 8057-8066,doi: 10.1021/acs.est.5b01236, 2015.

Atwater, M. A.: Radiative Effects of Pollutants in the Atmospheric Boundary Layer, J Atmos Sci, 28, 1367-1373, doi:10.1175/1520-0469(1971)028<1367:reopit>2.0.co;2, 1971.

Barbaro, E., Vilà-Guerau de Arellano, J., Krol, M. C., and Holtslag, A. A. M.: Impacts of Aerosol Shortwave Radiation Absorption on the Dynamics of an Idealized Convective Atmospheric Boundary Layer, Bound-Lay Meteorol. , 148, 31-49, doi:10.1007/s10546-013-9800-7, 2013.

Bi, J., Huang, J., Hu, Z., Holben, B. N., and Guo, Z.: Investigating the aerosol optical and radiative characteristics of heavy haze episodes in Beijing during January of 2013, J. Geophys. Res. Atmos., 119, 9884-9900, doi:10.1002/2014jd021757, 2014.

Bohren, C. F., and Huffman, D. R.: Absorption and scattering of light by small particles, Wiley Science Paperback Series, John Wiley & Sons, New York, NY, USA, 7, 7.5, 1983

Carslaw, K. S., Lee, L. A., Reddington, C. L., Pringle, K. J., Rap, A., Forster, P. M., Mann, G. W., Spracklen, D. V., Woodhouse, M. T., Regayre, L. A., and Pierce, J. R.: Large contribution of natural aerosols to uncertainty in indirect forcing, Nature, 503, 67-71, doi:10.1038/nature12674, 2013.

Curci, G., Ferrero, L., Tuccella, P., Barnaba, F., Angelini, F., Bolzacchini, E., Carbone, C., Denier Van Der Gon, H. A. C., Facchini, M. C., Gobbi, G. P., Kuenen, J. P. P., Landi, T. C., Perrino, C., Perrone, M. G., Sangiorgi, G., and Stocchi, P.: How much is particulate matter near the ground influenced by upper-level processes within and above the PBL? A summertime case study in Milan (Italy) evidences the distinctive role of nitrate, Atmos. Chem. Phys., 15, 2629-2649, doi:10.5194/acp-15-2629-2015, 2015.

Deng, X., Zhou, X., Tie, X., Wu, D., Li, F., Tan, H., and Deng, T.: Attenuation of ultraviolet radiation reaching the surface due to atmospheric aerosols in Guangzhou, Chin. Sci. Bull., 57, 2759-2766, doi:10.1007/s11434-012-5172-5, 2012.

Dickerson, R. R., Kondragunta, S., Stenchikov, G., Civerolo, K. L., Doddridge, B. G., and Holben, B. N.: The impact of aerosols on solar ultraviolet radiation and photochemical smog, Science, 278, 827-830, doi:10.1126/science.278.5339.827, 1997.

Ding, A. J., Fu, C. B., Yang, X. Q., Sun, J. N., Petäjä, T., Kerminen, V. M., Wang, T., Xie, Y., Herrmann, E., Zheng, L. F., Nie, W., Liu, Q., Wei, X. L., and Kulmala, M.: Intense atmospheric pollution modifies weather: a case of mixed biomass burning with fossil fuel combustion pollution in eastern China, Atmos. Chem. Phys., 13, 10545-10554, doi:10.5194/acp-13-10545-2013, 2013.

Ding, A. J., et al.: Enhanced haze pollution by black carbon in megacities in China, Geophys. Res. Lett., 43, 2873-2879, doi:10.1002/2016gl067745, 2016a.

Ding, A. J., et al.: Enhanced haze pollution by black carbon in megacities in China, Geophys. Res. Lett., 43, 2873-2879, doi:10.1002/2016GL067745, 2016b.

Fan, H., Zhao, C., and Yang, Y.: A comprehensive analysis of the spatio-temporal variation of urban air pollution in China during 2014–2018, Atmospheric Environment, 220, 117066, doi:10.1016/j.atmosenv.2019.117066, 2020.

Gan, C. M., Binkowski, F., Pleim, J., Xing, J., Wong, D., Mathur, R., and Gilliam, R.: Assessment of the aerosol optics component of the coupled WRF–CMAQ model using CARES field campaign data and a single column model, Atmospheric Environ. , 115, 670-682, doi: 10.1016/j.atmosenv.2014.11.028, 2015.

Gipson, G. L., and Young, J.: Process analysis, Science Algorithms of the EPA Models-3 Community Multiscale Air Quality (CMAQ) Modeling System, 1999.

Grell, G., Freitas, S. R., Stuefer, M., and Fast, J.: Inclusion of biomass burning in WRF-Chem: impact of wildfires on weather forecasts, Atmos. Chem. Phys., 11, 5289-5303, doi:10.5194/acp-11-5289-2011, 2011.

He, S., and Carmichael, G. R.: Sensitivity of photolysis rates and ozone production in the troposphere to aerosol properties, J. Geophys. Res. Atmos., 104, 26307-26324, doi:10.1029/1999jd900789, 1999.

Herman, J. R., Krotkov, N., Celarier, E., Larko, D., and Labow, G.: Distribution of UV radiation at the Earth's surface from TOMS-measured UV-backscattered radiances, J. Geophys. Res. Atmos., 104, 12059-12076, doi:10.1029/1999jd900062, 1999.

Hong, C., Zhang, Q., Zhang, Y., Davis, S. J., Zhang, X., Tong, D., Guan, D., Liu, Z., and He, K.: Weakening aerosol direct radiative effects mitigate climate penalty on Chinese air quality, Nat Clim Chang, 10, 845-850, doi:10.1038/s41558-020-0840-y, 2020.

Huang, W., Yang, Y., Wang, Y., Gao, W., Li, H., Zhang, Y., Li, J., Zhao, S., Yan, Y., Ji, D., Tang, G., Liu, Z., Wang, L., Zhang, R., and Wang, Y.: Exploring the inorganic and organic nitrate aerosol formation regimes at a suburban site on the North China Plain, Sci. Total Environ., 768, 144538, doi:10.1016/j.scitotenv.2020.144538, 2021.

Huang, X., Ding, A., Liu, L., Q., L., Ding, K., Nie, W., Xu, Z., Chi, X., Wang, M., Sun, J., Guo, W., and Fu, C. B.: Effects of aerosol-radiation interaction on precipitation during biomass-burning season in East China, Atmos. Chem. Phys., 16,10063-10082, doi:10.5194/acp-2016-272, 2016.

Huang, X., Wang, Z., and Ding, A.: Impact of Aerosol-PBL Interaction on Haze Pollution: Multiyear Observational Evidences in North China, Geophys. Res. Lett., 45, 8596-8603, doi:10.1029/2018GL079239, 2018.

Huang, X., and Ding, A.: Aerosol as a critical factor causing forecast biases of air temperature in global numerical weather prediction models, Sci. Bull., doi:10.1016/j.scib.2021.05.009, 2021.

Koch, D., and Del Genio, A. D.: Black carbon semi-direct effects on cloud cover: review and synthesis, Atmos. Chem. Phys., 10, 7685-7696, doi:10.5194/acp-10-7685-2010, 2010.

Li, C., Zhao, T., and Ying, K.: Effects of anthropogenic aerosols on temperature changes in China during the twentieth century based on CMIP5 models, Theor. Appl. Climatol., 125, 529-540, 2016.

Li, Z., Lee, K.-H., Wang, Y., Xin, J., and Hao, W.-M.: First observation-based estimates of cloud-free aerosol radiative forcing across China, J. Geophys. Res., 115, doi:10.1029/2009jd013306, 2010.

Li, Z., Guo, J., Ding, A., Liao, H., Liu, J., Sun, Y., Wang, T., Xue, H., Zhang, H., and Zhu, B.: Aerosol and Boundary-Layer Interactions and Impact on Air Quality, Natl. Sci. Rev.,4,810-833, doi:10.1093/nsr/nwx117, 2017.

Liao, H., Chang, W., and Yang, Y.: Climatic Effects of Air Pollutants over China: A Review, Adv. Atmos. Sci., 32, 115-139, doi:10.1007/s00376-014-0013-x, 2015.

Lim, S. S., et al.: A comparative risk assessment of burden of disease and injury attributable to 67 risk factors and risk factor clusters in 21 regions, 1990–2010: a systematic analysis for the Global Burden of Disease Study 2010, The Lancet, 380, 2224-2260, doi: 10.1016/S0140-6736(12)61766-8, 2012.

McCormick, R. A., and Ludwig, J. H.: Climate Modification by Atmospheric Aerosols, Science, 156, 1358-1359, doi:10.1126/science.156.3780.1358, 1967.

Mok, J., Krotkov, N. A., Arola, A., Torres, O., Jethva, H., Andrade, M., Labow, G., Eck, T. F., Li, Z., Dickerson, R. R., Stenchikov, G. L., Osipov, S., and Ren, X.: Impacts of brown carbon from biomass burning on surface UV and ozone photochemistry in the Amazon Basin, Sci. Rep., 6, 1-9, doi:10.1038/srep36940, 2016.

Pleim, J. E., and Xiu, A.: Development of a Land Surface Model. Part II: Data Assimilation, J Appl Meteorol Climatol, 42, 1811-1822, doi:10.1175/1520-0450(2003)042<1811:DOALSM>2.0.CO;2, 2003.

Pleim, J. E., and Gilliam, R.: An Indirect Data Assimilation Scheme for Deep Soil Temperature in the Pleim–Xiu Land Surface Model, J Appl Meteorol Climatol, 48, 1362-1376, doi:10.1175/2009JAMC2053.1, 2009.

Ramanathan, V., Crutzen, P. J., Kiehl, J. T., and Rosenfeld, D.: Aerosols, Climate, and the Hydrological Cycle, Science, 294, 2119-2124, doi:10.1126/science.1064034, 2001.

Ren, Y., Zhang, H., Zhang, X., Li, Q., Cai, X., Song, Y., Kang, L., and Zhu, T.: Temporal and spatial characteristics of turbulent transfer and diffusion coefficient of PM2.5, Sci. Total Environ., 782, 146804, doi:10.1016/j.scitotenv.2021.146804, 2021.

Rosenfeld, D., Sherwood, S., Wood, R., and Donner, L.: Atmospheric science. Climate effects of aerosol-cloud interactions, Science, 343, 379-380, doi:10.1126/science.1247490, 2014.

Sarwar, G., Luecken, D., Yarwood, G., Whitten, G. Z., and Carter, W. P.: Impact of an updated carbon bond mechanism on predictions from the CMAQ modeling system: Preliminary assessment, J Appl Meteorol Climatol, 47, 3-14, doi: 10.1175/2007JAMC1393.1, 2008.

Sun, Y. and Zhao, C.: Distinct impacts on precipitation by aerosol radiative effect over three different megacity regions of eastern China, Atmos. Chem. Phys., 21, 16555–16574, doi:10.5194/acp-21-16555-2021, 2021.

Wang, H., Xue, M., Zhang, X. Y., Liu, H. L., Zhou, C. H., Tan, S. C., Che, H. Z., Chen, B., and Li, T.: Mesoscale modeling study of the interactions between aerosols and PBL meteorology during a haze episode in Jing–Jin–Ji (China) and its nearby surrounding region – Part 1: Aerosol distributions and meteorological features, Atmos. Chem. Phys., 15, 3257-3275, doi:10.5194/acp-15-3257-2015, 2015.

Wang, H., Peng, Y., Zhang, X., Liu, H., Zhang, M., Che, H., Cheng, Y., and Zheng, Y.: Contributions to the explosive growth of PM2.5 mass due to aerosol–radiation feedback and decrease in turbulent diffusion during a red alert heavy haze in Beijing–Tianjin–Hebei, China, Atmos. Chem. Phys., 18, 17717-17733, doi:10.5194/acp-18-17717-2018, 2018a.

Wang, J., Xing, J., Mathur, R., Pleim, J. E., Wang, S., Hogrefe, C., Gan, C.-M., Wong, D. C., and Hao, J.: Historical trends in PM2. 5-related premature mortality during 1990–2010 across the northern hemisphere, Environ. Health Perspect., 125, 400-408, doi: 10.1289/EHP298, 2017.

Wang, J. D., Wang, S. X., Jiang, J. K., Ding, A. J., Zheng, M., Zhao, B., Wong, D. C., Zhou, W., Zheng, G. J., Wang, L., Pleim, J., and Hao, J. M.: Impact of aerosol–meteorology interactions on fine particle pollution during China's severe haze episode in January 2013, Environ. Res. Lett., 9, 094002, 2014.

Wang, S., Xing, J., Chatani, S., Hao, J., Klimont, Z., Cofala, J., and Amann, M.: Verification of anthropogenic emissions of China by satellite and ground observations, Atmospheric Environ., 45, 6347-6358, doi:10.1016/j.atmosenv.2011.08.054, 2011.

Wang, Z., Li, J., Wang, Z., Yang, W., Tang, X., Ge, B., Yan, P., Zhu, L., Chen, X., Chen, H., Wand, W., Li, J., Liu, B., Wang, X., Wand, W., Zhao, Y., Lu, N., and Su, D.: Modeling study of regional severe hazes over mid-eastern China in January 2013 and its implications on pollution prevention and control, Sci. China Earth Sci., 57, 3-13, doi:10.1007/s11430-013-4793-0, 2013.

Wang, Z., Huang, X., and Ding, A.: Dome effect of black carbon and its key influencing factors: a one-dimensional modelling study, Atmos. Chem. Phys., 18, 2821-2834, doi:10.5194/acp-18-2821-2018, 2018b.

Wendisch, M., Hellmuth, O., Ansmann, A., Heintzenberg, J., Engelmann, R., Althausen, D., Eichler, H., Müller, D., Hu, M., and Zhang, Y.: Radiative and dynamic effects of absorbing aerosol particles over the Pearl River Delta, China, Atmospheric Environ.., 42, 6405-6416, doi: 10.1016/j.atmosenv.2008.02.033, 2008.

Wong, D. C., Pleim, J., Mathur, R., Binkowski, F., Otte, T., Gilliam, R., Pouliot, G., Xiu, A., Young, J. O., and Kang, D.: WRF-CMAQ two-way coupled system with aerosol feedback: software development and preliminary results, Geosci. Model. Dev., 5, 299-312, doi:10.5194/gmd-5-299-2012, 2012.

Xing, J., Zhang, Y., Wang, S., Liu, X., Cheng, S., Zhang, Q., Chen, Y., Streets, D. G., Jang, C., Hao, J., and Wang, W.: Modeling study on the air quality impacts from emission reductions and atypical meteorological conditions during the 2008 Beijing Olympics, Atmospheric Environ. , 45, 1786-1798, doi:10.1016/j.atmosenv.2011.01.025, 2011.

Xing, J., Mathur, R., Pleim, J., Hogrefe, C., Gan, C.-M., Wong, D. C., Wei, C., and Wang, J.: Air pollution and climate response to aerosol direct radiative effects: A modeling study of decadal trends across the northern hemisphere, J. Geophys. Res. Atmos., 120, 12,221-12,236, doi:10.1002/2015JD023933, 2015a.

Xing, J., Mathur, R., Pleim, J., Hogrefe, C., Gan, C. M., Wong, D. C., and Wei, C.: Can a coupled meteorology–chemistry model reproduce the historical trend in aerosol direct radiative effects over the Northern Hemisphere?, Atmos. Chem. Phys., 15, 9997-10018, doi:10.5194/acp-15-9997-2015, 2015b.

Xing, J., Wang, J., Mathur, R., Pleim, J., Wang, S., Hogrefe, C., Gan, C.-M., Wong, D. C., and Hao, J.: Unexpected Benefits of Reducing Aerosol Cooling Effects, Environ. Sci. Technol., 50, 7527-7534, doi:10.1021/acs.est.6b00767, 2016.

Xing, J., Wang, J., Mathur, R., Wang, S., Sarwar, G., Pleim, J., Hogrefe, C., Zhang, Y., Jiang, J., Wong, D. C., and Hao, J.: Impacts of aerosol direct effects on tropospheric ozone through changes in atmospheric dynamics and photolysis rates, Atmos. Chem. Phys. Discuss., 2017, 1-24, doi:10.5194/acp-2017-198, 2017.

Yang, X., Zhao, C., Guo, J., and Wang, Y.: Intensification of aerosol pollution associated with its feedback with surface solar radiation and winds in Beijing, J. Geophys. Res. Atmos., 121, 4093–4099, doi:10.1002/2015JD024645, 2016a.

Yang, X., Zhao, C., Zhou, L., Li, Z., Cribb, M., and Yang, S.: Wintertime cooling and a potential connection with transported aerosols in Hong Kong during recent decades, Atmospheric Research, 211, 52–61, doi:10.1016/j.atmosres.2018.04.029, 2018.

Yang, X., Zhao, C., Zhou, L., Wang, Y., and Liu, X.: Distinct impact of different types of aerosols on surface solar radiation in China: Variation of Aerosol Radiative Effect, J. Geophys. Res. Atmos., 121, 6459–6471, doi:10.1002/2016JD024938, 2016b.

Yang, Y., Russell, L. M., Lou, S., Liao, H., Guo, J., Liu, Y., Singh, B., and Ghan, S. J.: Dust-wind interactions can intensify aerosol pollution over eastern China, Nat. Commun., 8,1-8, doi:10.1038/ncomms15333, 2017.

Zhang, K., Zhao, C., Fan, H., Yang, Y., and Sun, Y.: Toward Understanding the Differences of PM2.5 Characteristics Among Five China Urban Cities, Asia-Pacific J Atmos Sci, 56, 493–502, doi:10.1007/s13143-019-00125-w, 2020.

Zhao, B., Wang, S., Wang, J., Fu, J. S., Liu, T., Xu, J., Fu, X., and Hao, J.: Impact of national NOx and SO2 control policies on particulate matter pollution in China, Atmospheric Environ., 77, 453-463, doi:10.1016/j.atmosenv.2013.05.012, 2013a.

Zhao, B., Wang, S. X., Dong, X. Y., Wang, J. D., Duan, L., Fu, X., Hao, J. M., and Fu, J.: Environmental effects of the recent emission changes in China: implications for particulate matter pollution and soil acidification, Environ. Res. Lett., 8, 024031, doi:10.1088/1748-9326/8/2/024031, 2013b.

Zhao, C., Lin, Y., Wu, F., Wang, Y., Li, Z., Rosenfeld, D., and Wang, Y.: Enlarging Rainfall Area of Tropical Cyclones by Atmospheric Aerosols, Geophys. Res. Lett., 45, 8604–8611, doi:10.1029/2018GL079427, 2018.

Zhao, C., Yang, Y., Fan, H., Huang, J., Fu, Y., Zhang, X., Kang, S., Cong, Z., Letu, H., and Menenti, M.: Aerosol characteristics and impacts on weather and climate over the Tibetan Plateau, 7, 492–495, doi:10.1093/nsr/nwz184, 2020.

Zheng, G. J., Duan, F. K., Su, H., Ma, Y. L., Cheng, Y., Zheng, B., Zhang, Q., Huang, T., Kimoto, T., Chang, D., Poschl, U., Cheng, Y. F., and He, K. B.: Exploring the severe winter haze in Beijing: the impact of synoptic weather, regional transport and heterogeneous reactions, Atmos. Chem. Phys., 15, 2969-2983, doi:10.5194/acp-15-2969-2015, 2015.

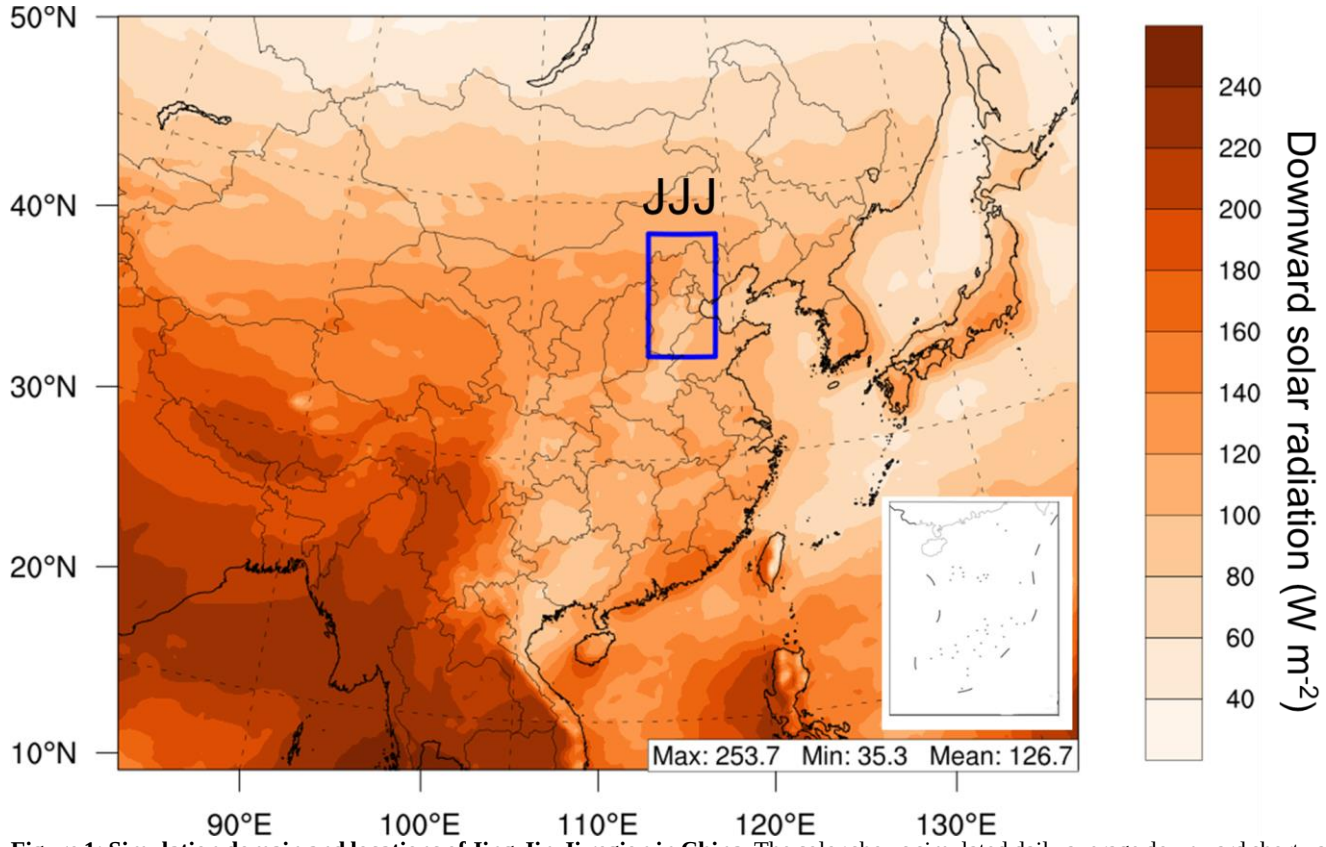

Figure 1: Simulation domain and locations of Jing-Jin-Ji region in China. The color shows simulated daily average downward shortwave solar radiation (SWDOWN) at bottom in January, 2013

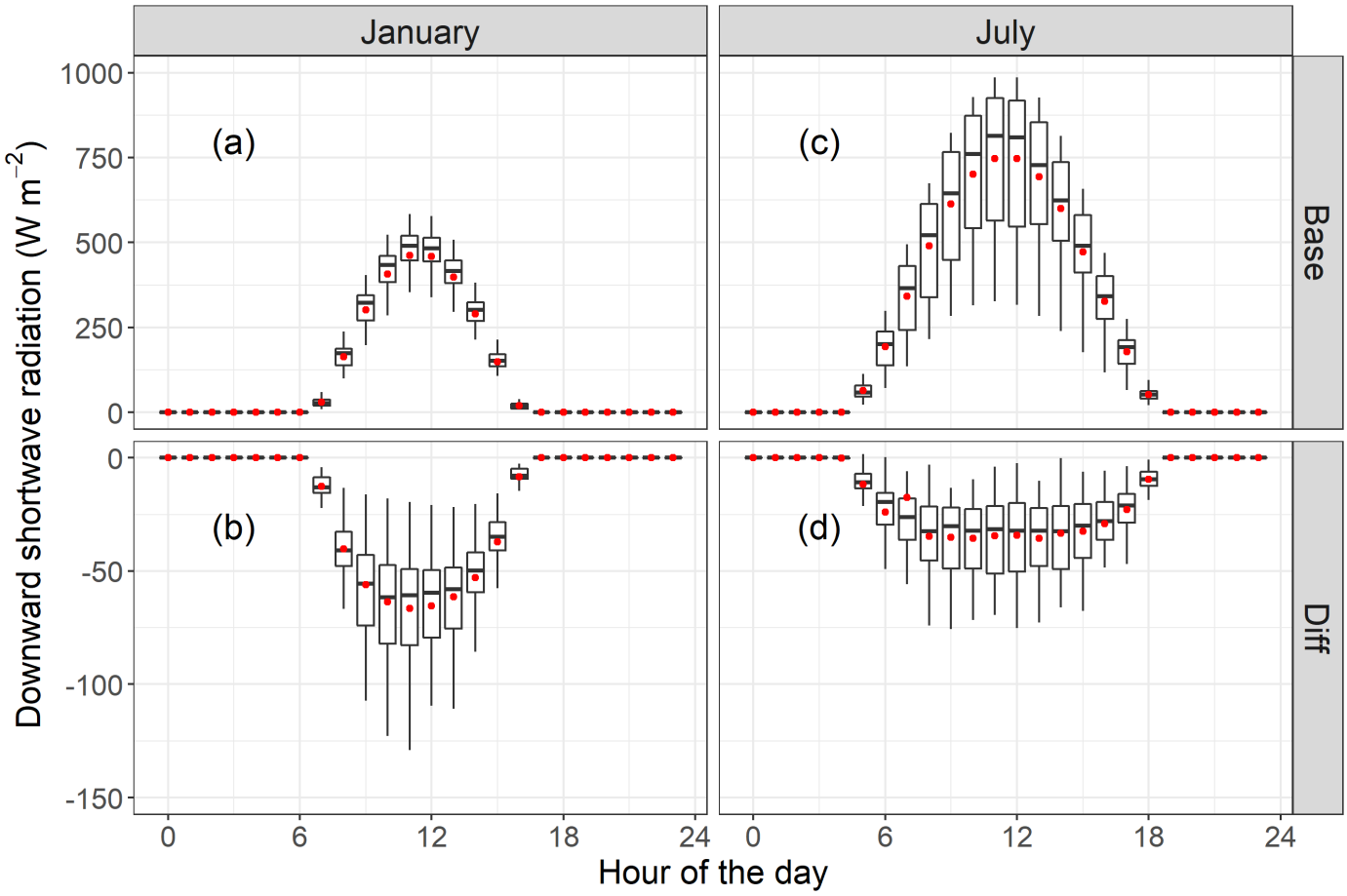

390

Figure 2: Diurnal variances of SWDOWN (a and c) and the impact of ADE on SWDOWN (b and d), in January and July 2013. The central rectangle spans the first quartile to the third quartile. The segment and red dot inside the rectangle show the median and mean value, respectively. The whiskers above and below the box extend to the highest and lowest values.

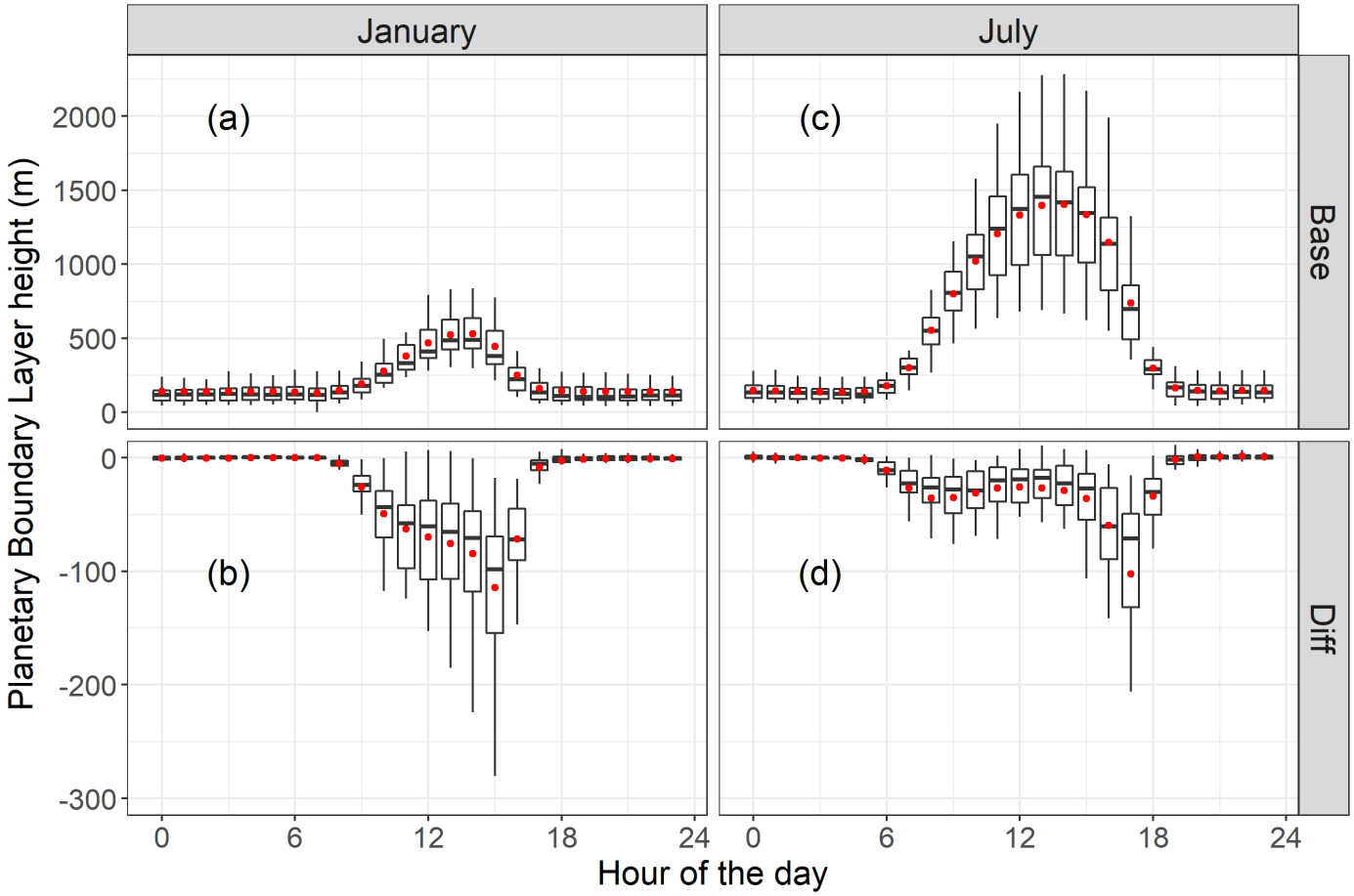

Figure 3: Diurnal variances of Planetary Boundary Layer (PBL) height (a and c) and the impact of ADE on PBL height (b and d), in January and July, 2013. The central rectangle spans the first quartile to the third quartile. The segment and red dot inside the rectangle show the median and mean value, respectively. The whiskers above and below the box extend to the highest and lowest values.

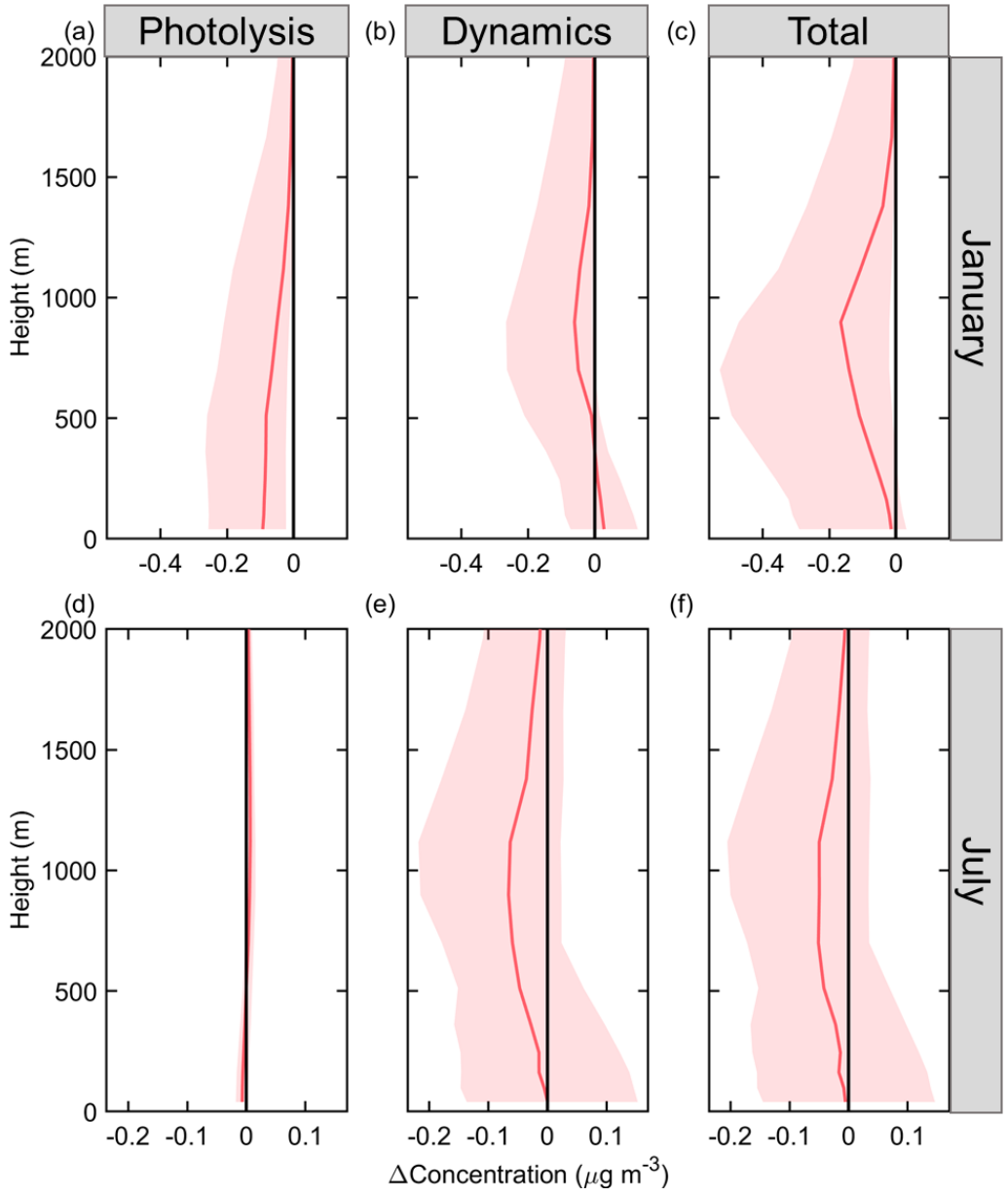

Figure 4: Vertical profile of sulfate concentration change to ADE in JJJ region at noontime in January (a b c) and July (d e f).

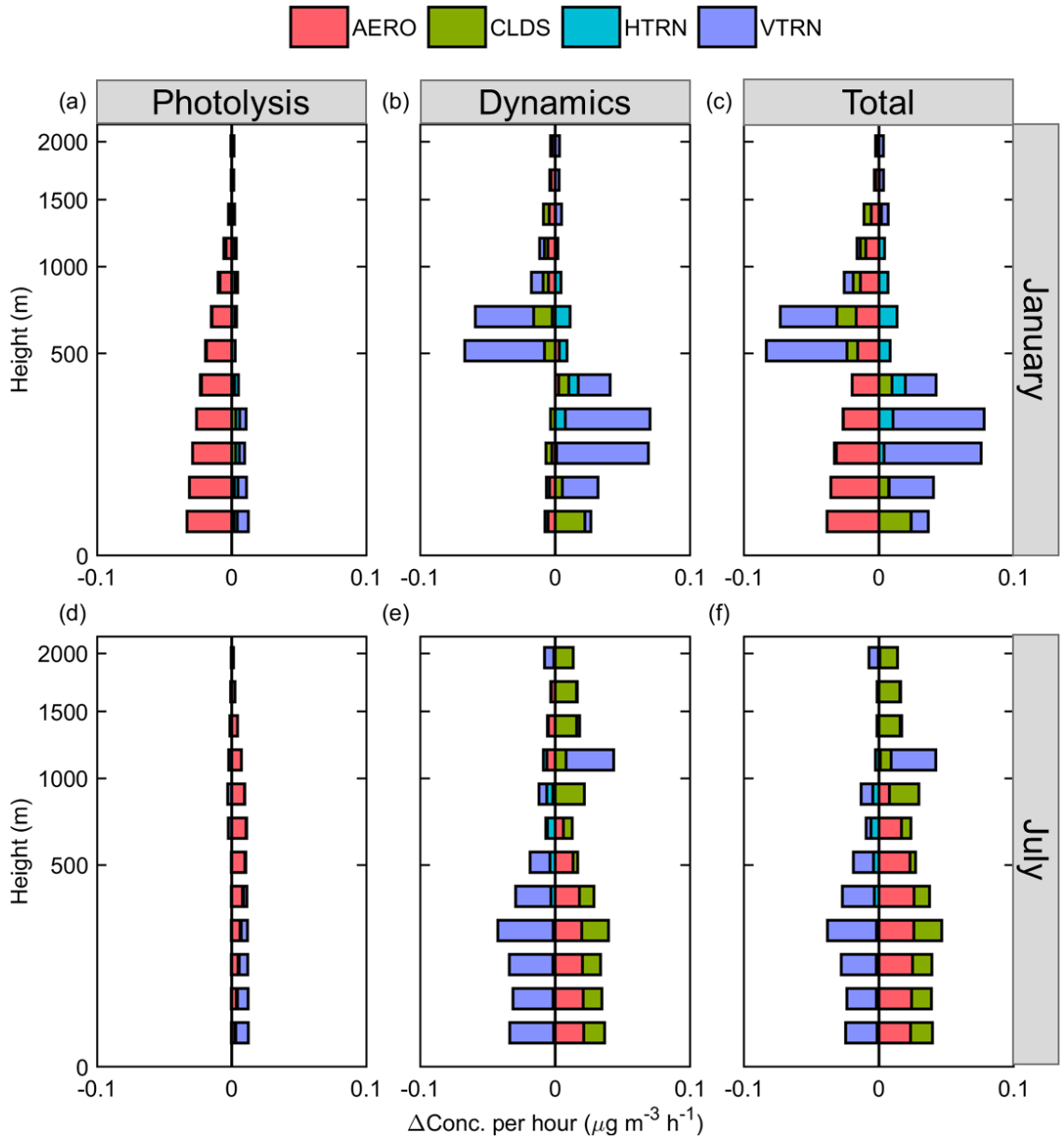

Figure 5: Vertical distribution the responses of main process of sulfate to ADE in JJJ region at noontime in January (a b c) and July (d e f).

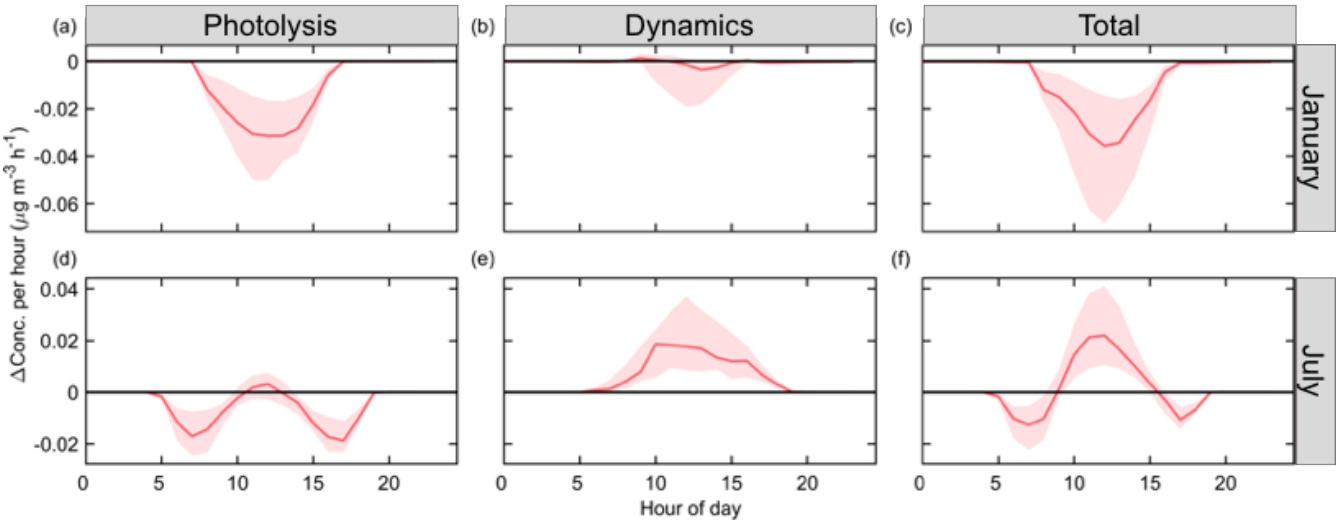

Figure 6: **Diurnal variances of ADE impact on AERO of sulfate in January and July.** The red line and shadow depict the medium value and 25th to 75th percentiles, respectively.

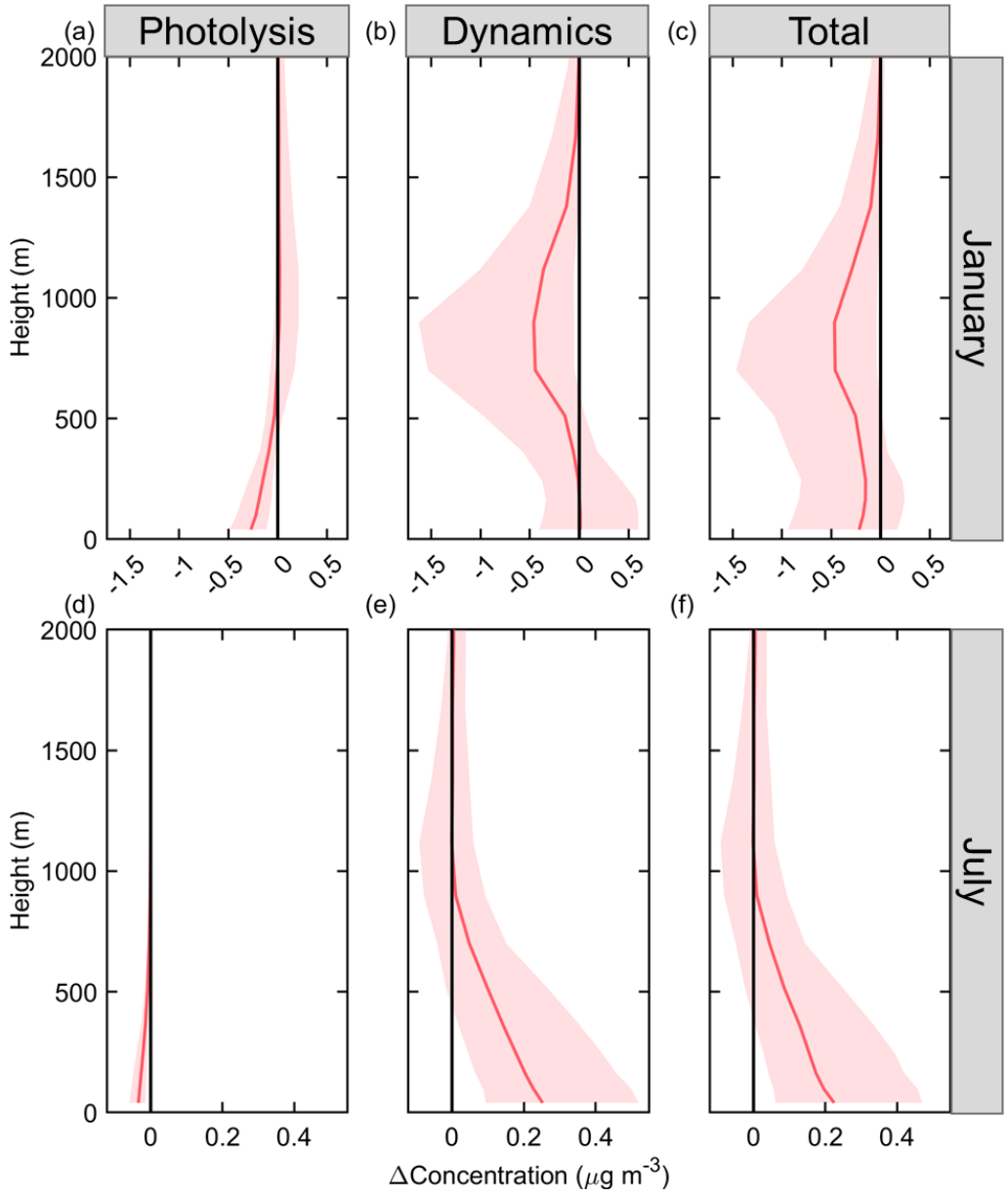

Figure 7: Vertical profile of nitrate concentration change to ADE in JJJ region at noontime in January (a b c) and July (d e f).

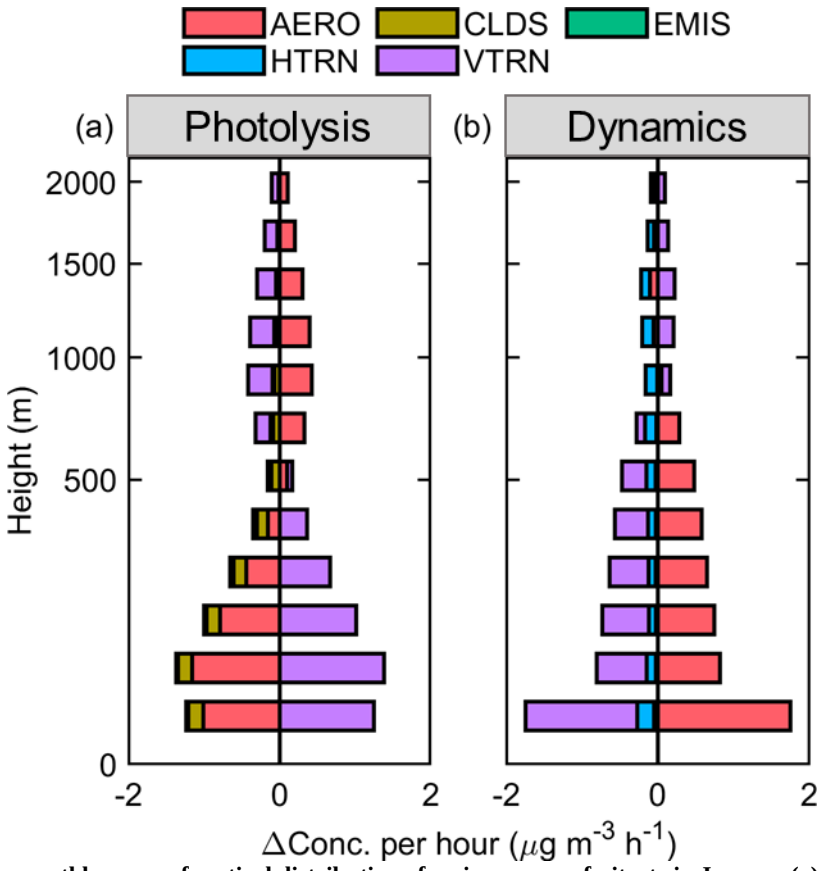

Figure 8: The monthly mean of vertical distribution of main process of nitrate in January (a) and July (b).

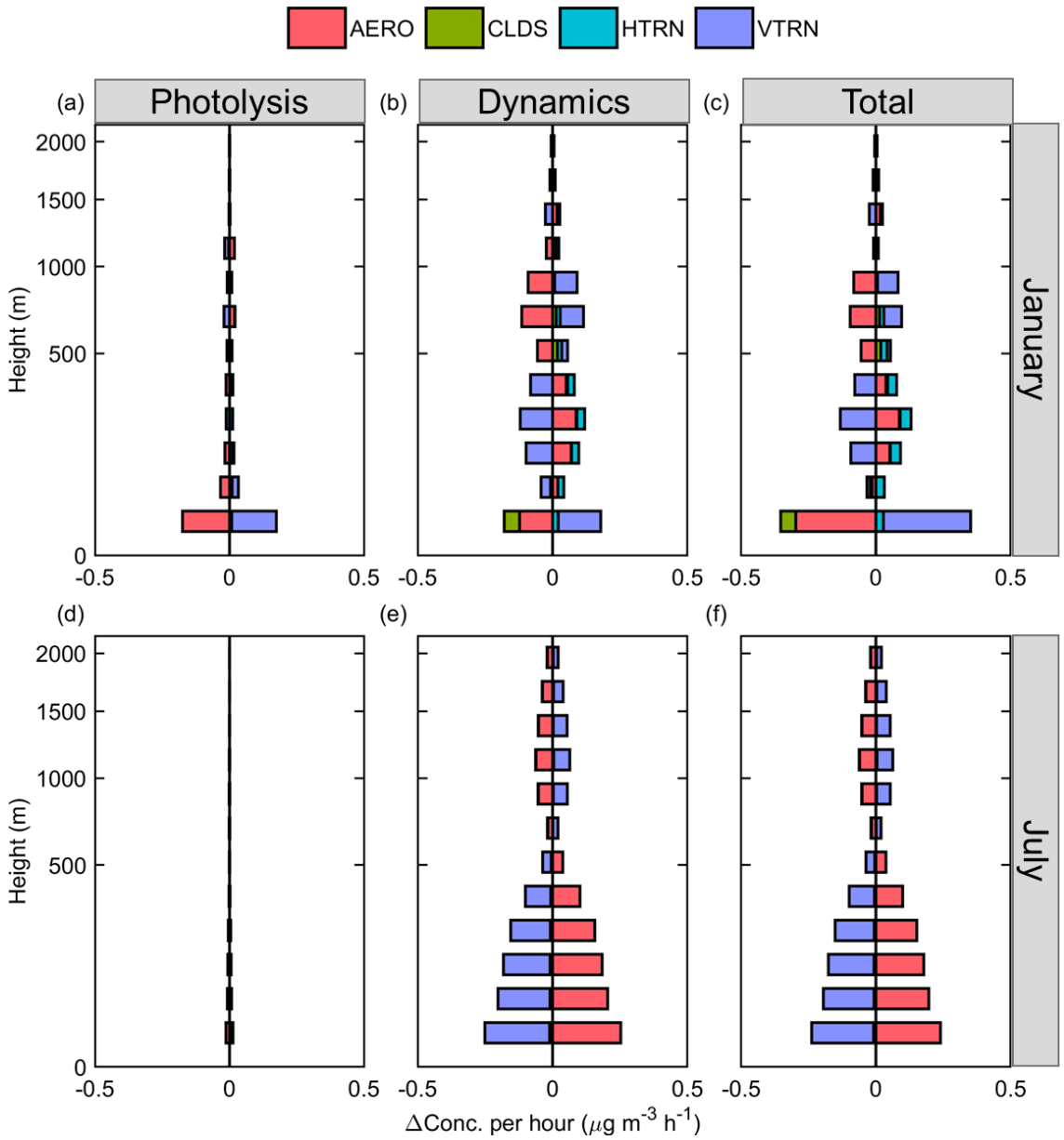

Figure 9: Vertical distribution the responses of main process of nitrate to ADE in Jing-Jin-Ji(JJJ) region in January (a b c) and July (d e f).